Chemosphere 298 (2022) 134238

Contents lists available at ScienceDirect

Chemosphere

journal homepage: www.elsevier.com/locate/chemosphere

Aging of microplastics increases their adsorption affinity towards organic contaminants

Kartik Bhagat [a], Ana C. Barrios [a], Kimya Rajwade [a], Abhishek Kumar [a], Jay Oswald [b], Onur Apul [c], François Perreault [a,*]

[a] School of Sustainable Engineering and the Built Environment, Arizona State University, USA
[b] School of Engineering of Matter, Transport and Energy, Arizona State University, USA
[c] Department of Civil and Environmental Engineering, University of Maine, Orono, USA

HIGHLIGHTS

- An experimental approach to mimic environmental microplastics was developed.
- Microplastics were aged with ultraviolet light with or without hydrogen peroxide.
- Aging was expressed quantitatively through carbonyl indices and percentage oxygen.
- Adsorption of phenanthrene and methylene blue was higher on aged microplastics.
- Methylene blue showed greatest increase in adsorption after microplastics aging.

GRAPHICAL ABSTRACT

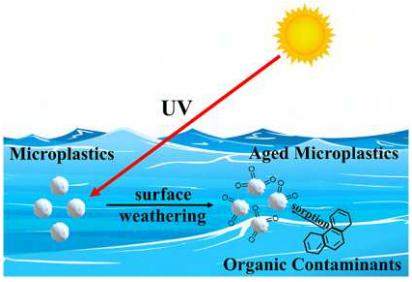

ARTICLE INFO

Handling Editor: Michael Bank

Keywords:
Surface weathering
Carbonyl index
Organic contaminant
Adsorption

ABSTRACT

When released in the environment, microplastics undergo surface weathering due to mechanical abrasion and ultraviolet exposure. In this study, the adsorption of two model contaminants, phenanthrene and methylene blue, by weathered high density polyethylene (HDPE) and polypropylene (PPE) was evaluated to understand how the microplastics' aging influences contaminant adsorption. Microplastics were aged through an accelerated weathering process using ultraviolet exposure with or without hydrogen peroxide. Adsorption isotherms were conducted for both contaminants on pristine and aged microplastics. The adsorption of organic contaminants was higher on aged microplastics than on pristine ones, with methylene blue having the highest affinity increase with aging at 4.7-fold and phenanthrene having a 1.9-fold increase compared to the pristine particles. To understand the mechanisms involved with higher adsorption of contaminants by aged microplastics, changes in the specific surface area and surface chemistry of aged microplastics were characterized by Fourier Transform Infrared Spectroscopy, X-ray Photoelectron Spectroscopy, zeta potential, X-ray tomography, and Brunauer–Emmett–Teller krypton adsorption analyses. The results of this study show that oxidation of microplastics can enhance the adsorption of organic contaminants, which may increase their role as vectors of contaminants in the aquatic food chain.

* Corresponding author. College Avenue Commons (CAVC) Building, 660 S. College Avenue, #507, Tempe, AZ, 85281, USA.
E-mail address: francois.perreault@asu.edu (F. Perreault).

https://doi.org/10.1016/j.chemosphere.2022.134238
Received 26 December 2021; Received in revised form 26 February 2022; Accepted 4 March 2022
Available online 8 March 2022

1. Introduction

Plastic products are economical, lightweight and versatile, which has resulted in their widespread use in consumer products (Geyer et al., 2017). The global plastic production in 2015 was estimated at about 381 million tons, which is a nearly 200-fold increase from 1950 (Ritchie and Roser, 2018). With such mass production of plastics, their disposal has become a challenge and there is evidence that plastics find their way into the oceans, lakes, and other water bodies (Cole et al., 2011; Thompson et al., 2004). Due to their durability, plastics will persist and accumulate in the aquatic ecosystems for decades (Worm et al., 2017). However, the environmental implications of this growing mass of plastic pollution are still hard to predict.

In the environment, plastics degrade under the action of mechanical and abrasive forces (Andrady, 2011; Barnes et al., 2009). This leads to the formation of smaller fragments called microplastics, which are broadly categorized as any plastic particles with a size below 5 mm. Microplastics are a source of many concerns due to their potential interactions with aquatic organisms, including the ability to enter the aquatic food chain (*GESAMP*, 2015; Revel et al., 2018; Wright et al., 2013). Previous studies have shown that microplastics can be a sink for organic contaminants due to the high affinity of organic contaminants towards the hydrophobic plastic surface (Lee et al., 2014). When present in a mixture of contaminants, microplastics can have synergistic or antagonistic interactions that will affect the overall toxicity of the mixture (Bhagat et al., 2021; Koelmans et al., 2016; Teuten et al., 2009). For example, Setälä et al. investigated the transfer of these organic leachates by microplastics to microzooplankton and showed that microplastics, without undergoing biodegradation, released the adsorbed chemicals in the zooplankton's gut (Setälä et al., 2014). Alvarez-Ruiz showed higher bioconcentration factors of perfluoroalkyl substances in mussels when microplastics were present in the mixture but noted the opposite effect of lower bioconcentration for the pesticides terbuthylazine and chlorpyrifos when co-exposed with microplastics (Álvarez-Ruiz et al., 2021). In *in vitro* cell cultures, Rubin and Zucker demonstrated an augmented joint toxicity of triclosan adsorbed on microplastics towards Caco-2 cells due to the adsorption of triclosan on the microplastics in the aqueous environment and its subsequent desorption in the cell (Rubin and Zucker, 2022). Therefore, understanding the interactions of microplastics with contaminants will be critical in our ability to predict the environmental implications of microplastics.

However, the surface chemistry of microplastics also evolves in the environment under the effect of sunlight. Ultraviolet (UV) irradiation alters the polymer structure by introducing hydro-peroxides and oxygen-containing functional groups, which leads to chain scission (Pandey and Singh, 2001). Therefore, the chemistry of the microplastics found in the environment will be different from the plastic models commonly used in laboratory studies, which are often pristine particles with uniform shapes and sizes (Ngoc et al., 2016; Rubin et al., 2021a). By changing the surface properties of microplastics, aging can also alter their environmental interactions. Vroom et al. showed that aging of polystyrene microplastics increases their ingestion by zooplankton (Vroom et al., 2017) while Huffer et al. showed that the adsorption affinity of polystyrene microplastics for different organic compounds decreases with aging (Hüffer et al., 2018). However, only one type of microplastic was investigated and the authors noted that the adsorption of organic contaminants with one type of microplastic does not predict the fate of all microplastics. Moreover, bead shaped polystyrene microplastics lack environmental significance compared to real microplastics (Lowry et al., 2020; Rubin et al., 2021). Therefore, there is a need to better understand how microplastic aging will affect environmental fate for a wider range of microplastic models.

In the present study, we investigated the effect of surface weathering on the affinity of two common environmental microplastics, high-density polyethylene (HDPE) and polypropylene (PPE), with organic contaminants. Surface weathering caused by UV irradiation and surface oxidation led to changes in the surface chemistry and morphology of the microplastics, which were measured by Fourier Transformed Infrared Spectroscopy (FT-IR), X-ray electron Spectroscopy (XPS), X-ray tomography, and Brunauer–Emmett–Teller (BET) surface area analyses. The physico-chemical properties of the aged microplastic particles were compared with real environmental microplastics to confirm the environmental relevance of the microplastic models generated. Using methylene blue (MB) and phenanthrene as model contaminants, we compared the adsorption of aged and pristine microplastics. Our results show that surface weathering increases the adsorption of organic contaminants by microplastics. These findings have important implications for both the environmental fate of contaminants when in the presence of microplastics and the potential hazard of microplastics as a vector of micropollutants.

2. Materials and methods

2.1. Materials

Plastics were purchased in the form of sheets (1/8" × 12" × 12") from King Plastic Corporation (Florida, USA). The plastics used in this study, HDPE and PPE, were selected because they constitute the two most commonly produced and disposed plastics worldwide. Phenanthrene ($C_{14}H_{10}$, 98%), a priority pollutant for the Environmental Protection Agency, and MB ($C_{16}H_{18}ClN_3S$, >99%), a common model for adsorption studies, were obtained from Sigma-Aldrich (St. Louis, MO, USA). The physical and chemical properties of the sorbates are listed in Table S1, as well as details on the preparation of stock solutions.

2.2. Preparation and aging of microplastic particles

For the preparation of the microplastics, small pieces (~2 cm^2) were cut from HDPE or PPE sheets, weighed up to 50 g, mixed with 50 mL deionized (DI) water, and blended for 15 min in a stainless-steel blender. The temperature in the blending solution did not rise above 65°C. Aging of the resulting microplastic particles was done in a UV-ozone chamber (Bioforce Nanosciences, IA, USA) with a wavelength of 254 nm and UV intensity of 19.39 mW/cm^2 at a distance of 0.437 inches. This irradiation is ~2.8 times the solar irradiation in the UV range. The microplastics (HDPE or PPE) were kept in the chamber for 4 h with DI water or 4 h with H_2O_2 (diluted to 10% v/v). The addition of H_2O_2 accelerates the aging process by the formation of hydroxyl radicals that enhanced surface oxidation, as described by Huffer et al. for the aging of polystyrene (Hüffer et al., 2018). After aging, the particles were washed with DI water and dried at room temperature.

2.3. Characterization of microplastic particles

The size distribution of the microplastics was analyzed by dry sieving through a series of metal sieves (mesh number 18, 50, 140, and 325; McMaster Carr, Princeton, NJ). The morphology of the microplastics was characterized by image analysis of pictures taken by a digital camera or, for the smallest particle size, with a Leica DM6 bright field microscope (Leica Microsystems Inc., Buffalo Grove, IL). Particle size distribution was determined by image analysis of 5 different pictures using ImageJ (National Institutes of Health, MD).

For the characterization of microplastics, samples were vacuum dried for at least 1 week before use. The microplastics' surface composition was analyzed using XPS on a VG 220i-XL (Thermo Fisher Scientific Ltd. Hampton, NH) equipped with a monochromated Al K-alpha X-ray source. The XPS data analysis was done using the CasaXPS software (version 2.3.18). For FT-IR, analyses were performed on a Bruker IFS66 V/S FT-IR system equipped with a mercury cadmium telluride standard detector and a KBr beam splitter with a diamond attenuated total reflectance module. The carbonyl index was calculated as the

absorbance ratios for the C═O detection wavelength at 1716 cm^{-1} and C–H_3 detection wavelength at 720 cm^{-1} (Benítez et al., 2013) and 972 cm^{-1} (Andreassen, 1999) for HDPE and PPE, respectively, as follows:

$$\text{Carbonyl Index} = \frac{A(1716)}{A(720)} \quad (1)$$

Computed X-ray tomography images of pristine and aged HDPE microplastics were obtained using a ZEISS Xradia 520 Versa submicron X-ray imaging system. A cone shape X-ray beam with a transmitted voltage of 40.13 kV produced 997 images of the sample that underwent a 360° rotation (3 μm/voxel), The microscope objective was 4X and the cone angle was 3.39°. The raw data was analyzed using VG Studio Max software (Volume Graphics, Germany) to calculate the defect volume percentage or porosity by selecting regions of interest (ROI) representative of the whole sample.

Additional methodology for microplastic characterization using B.E.T. krypton adsorption analysis, streaming zeta potential, and Raman spectroscopy can be found in the SI.

2.4. Adsorption experiments

Adsorption experiments were performed as previously described (Bakir et al., 2014; Hameed et al., 2007), with the following modifications. The MB adsorption experiments were carried out in 10 mL acid-cleaned glass vials with 300 mg of pristine or aged microplastics and 10 mL of DI water with different concentrations of MB (2–32 mg/L). For phenanthrene (0.0625–1 mg/L), 50 mg of pristine or aged microplastics were added into 10 mL glass vials without any headspace. Bottles were spiked with predetermined volumes of phenanthrene from its methanol stock solution (96 mg/L). Methanol concentration was kept below 0.1% (v/v) to avoid co-solvent interactions (Bakir et al., 2012). The bottles were shaken at 9 rpm for 5 h in the case of MB, and 48 h in the case of phenanthrene at 25 °C. Positive control bottles without plastic were run in parallel to correct for possible loss due to adsorption to the vial, while negative control bottles with plastic and no contaminant were run to correct for possible leaching of chemicals from microplastics. At the respective equilibrium time for each contaminant, the supernatant was collected using a 0.45 μm syringe filter (VWR International) and analyzed in a microplate reader (BioTek, Synergy). MB was measured by absorption at 608 nm whereas phenanthrene was quantified by fluorescence using an excitation wavelength of 252 nm and an emission wavelength of 370 nm. Calibration curves were made for each compound to convert the absorbance and fluorescence intensity values to concentrations. The isotherms obtained were modelled as per Langmuir and Freundlich (model equations are shown in the SI) to find the best experimental fit in the Origin Pro, 2018 (64-bit) software. The mass of contaminants adsorbed to microplastics at equilibrium time, q_e, was calculated as follows:

$$q_e = \frac{(C_o - C_e)\cdot V}{W} \quad (2)$$

Where, q_e is the adsorbed amount in (mg/g), C_o and C_e (mg/L) are the liquid-phase concentrations of MB and phenanthrene at initial and equilibrium state, respectively. V (L) is the volume of solution and W (g/L) is the dosage of microplastics used.

3. Results and Discussion

3.1. Microplastics characterization

Fig. 1A shows the size distribution of the two microplastics generated in this work. Fig. 1B and D shows the portion of microplastics left in sieve #18 (>1 mm) for HDPE and PPE, respectively, while Fig. 1C and E shows the bright-field microscopy images of HDPE and PPE, respectively, sieved out from the sieve #140 (between 0.105 and 0.297 mm). The percentage weight distribution for each sieve fraction, shown in Table S2, indicates that over 99.9% of the weight used was recovered during the sieve analysis. The average particle size of the HDPE and PPE microplastics, calculated from Fig. 1A, was 0.530 mm and 0.545 mm, respectively. The size distribution obtained was similar to the size range of microplastics found during field sampling studies (Desforges et al., 2014; Eriksen et al., 2013; Gajšt et al., 2016; Kanhai et al., 2017; Klein et al., 2015), as shown on Figure S1. Therefore, the procedure developed was able to produce a microplastic material with a size distribution representative of environmental microplastics.

3.2. Change in surface chemistry during microplastics aging

Microplastics were characterized by FT-IR and Raman spectroscopy to determine how weathering changed their chemical structure. The FT-IR spectra of the pristine microplastics confirm their chemical nature. The HDPE microplastics show characteristic peaks at 1470 cm^{-1} and 720 cm^{-1} associated with the C–H bending of CH_2 bonds and rocking mode of CH_3 bonds of HDPE (Benítez et al., 2013), while PPE has signature peaks at 1460 cm^{-1} and 1380 cm^{-1} for the symmetric bending of CH_3 bonds, and 972 cm^{-1} for CH_3 rocking bonds (Andreassen, 1999) as shown in Fig. 2A and B. After surface weathering, the FT-IR spectra of both HDPE and PPE show indications of polymer oxidation (Fig. 4A and B). Photo-oxidation of polymers occurs when UV radiation is absorbed

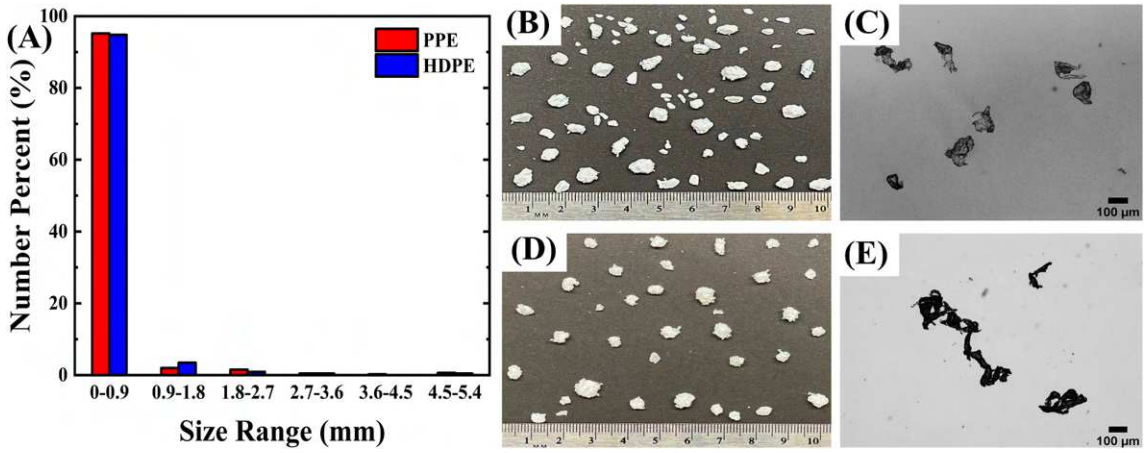

Fig. 1. (A) Size distribution of the microplastics. (B) Visual analysis of microplastics collected on sieve # 18, with a ruler included for size analysis for HDPE. (C) Bright field imaging (40X magnification) of microplastics collected on sieve # 140 for HDPE. (D) Visual analysis of microplastics collected on sieve #18, with a ruler included for size analysis for PPE. (E) Bright field imaging (40X magnification) of microplastics collected on sieve # 140 for PPE.

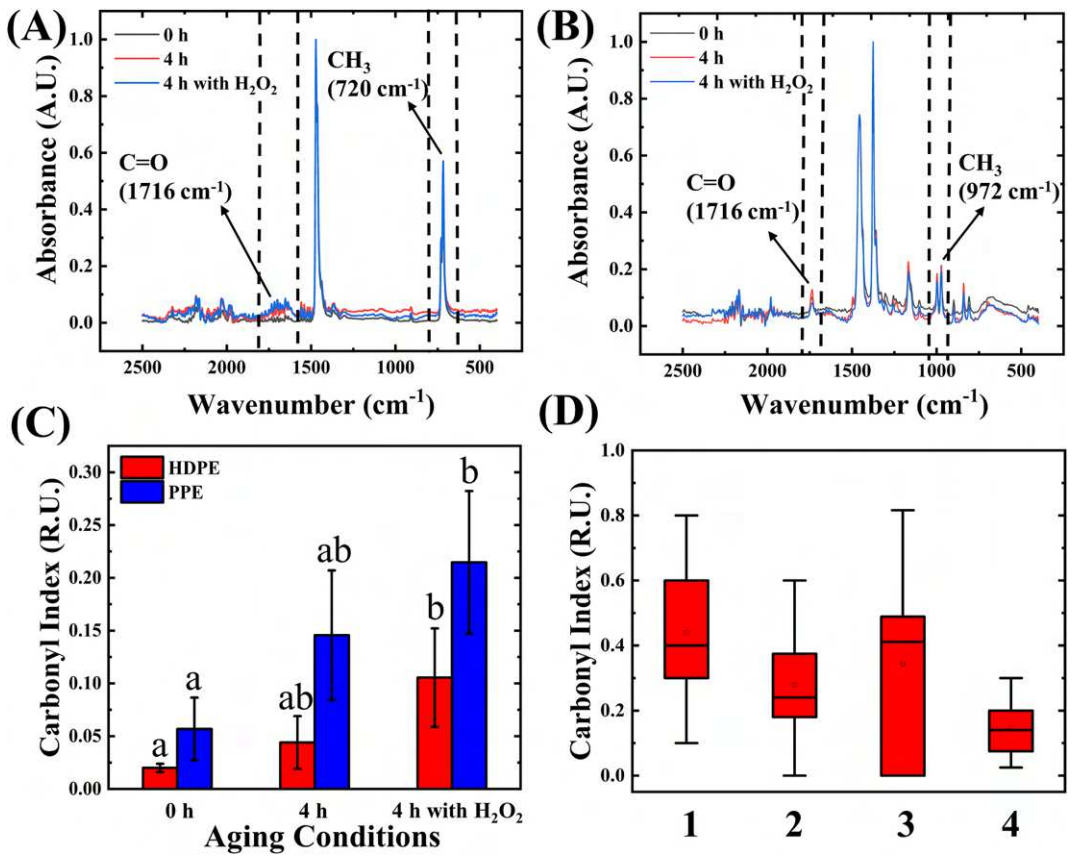

Fig. 2. (A) FT-IR spectra of pristine and aged HDPE microplastics, (B) FT-IR spectra of pristine and aged PPE microplastics, (C) Carbonyl indices obtained from FT-IR analyses. Letters above bars indicate statistical difference ($p < 0.05$) according to ANOVA followed by a Tukey HSD test ($n = 3$) and (D) Carbonyl indices of real environmental microplastics reported by 1- (Halle et al., 2017), 2- (Veerasingam et al., 2016), and 3- (Sarkar et al., 2021) compared to 4- the carbonyl indices obtained in this study.

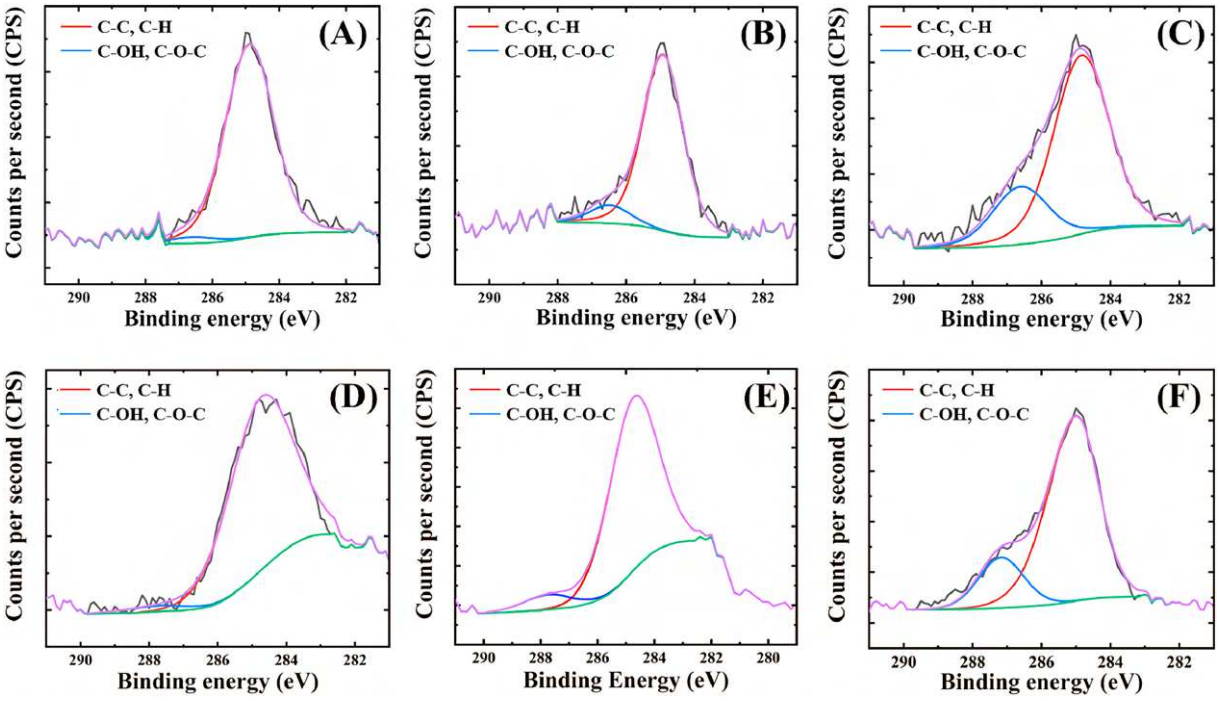

Fig. 3. XPS C1s deconvolution spectra for (A) HDPE 0 h, (B) HDPE 4 h, (C) HDPE 4 h with H_2O_2, (D) PPE 0 h, (E) PPE 4 h, and (F) PPE 4 h with H_2O_2.

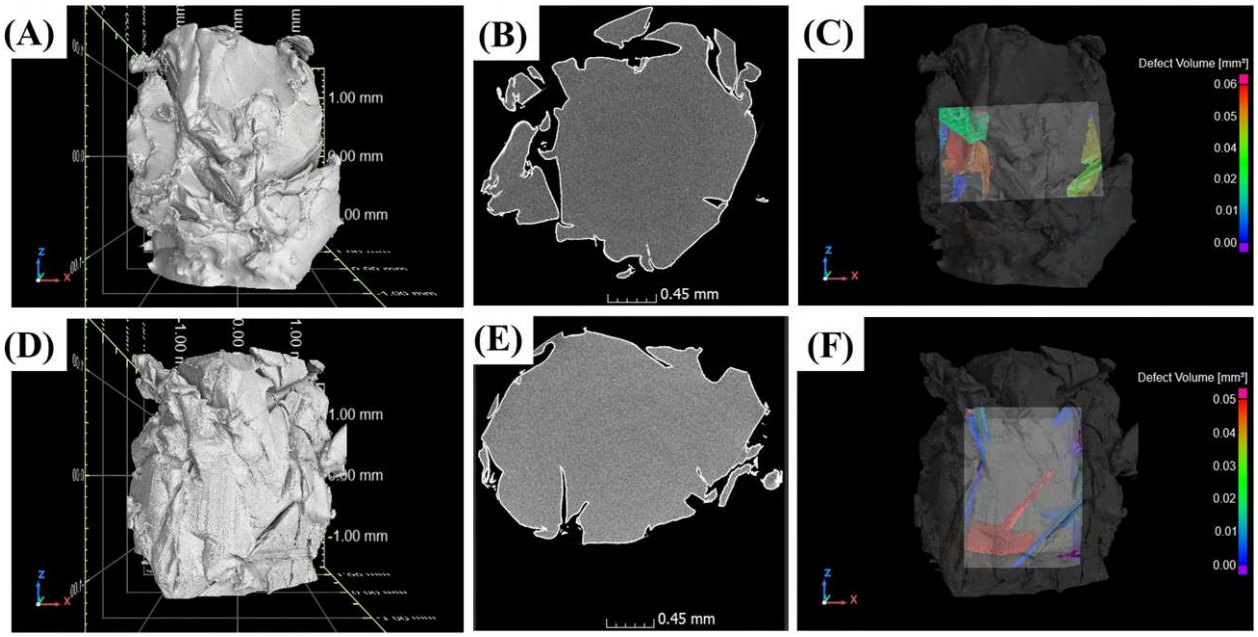

Fig. 4. X-ray tomographic images of pristine and aged HDPE microplastics. (A) 3-D volume reconstructed of pristine HDPE microplastics, (B) Top projection of pristine HDPE microplastic, (C) Visualization of defect volume using cuboidal region of interest for porosity calculation of pristine HDPE microplastic (2.4% ± 0.6%, n = 3)), (D) 3-D volume reconstructed of aged HDPE microplastic, (E) Top projection of aged HDPE microplastic and, (F) Visualization of defect volume using cuboidal region of interest for porosity calculation of aged HDPE microplastic (1.5% ± 0.2%, n = 3).

by the material, which results in the formation of free radicals and the scission of C–H bonds. After free radicals are formed, hydroperoxides are generated by reaction with oxygen (Brandon et al., 2016; ter Halle et al., 2017; Wypych, 2013), which further decompose into a variety of products, such as aldehydes and alkenes. This process is accelerated by the addition of H_2O_2, which also reacts with UV to provide an external source of free radicals. Surface oxidation that leads to the formation of functional groups such as carbonyl groups, esters and gamma-lactones, which have oscillations in the 1780-1684 cm^{-1} region (Hüffer et al., 2018). The increasing intensity of these peaks in both HDPE and PPE (Fig. 2A and B) exposed to UV or UV + H_2O_2 confirms the weathering of microplastics. Microplastic weathering is also supported by Raman spectroscopy (shown in Figure S2 of the SI), where the weakening of the Raman signal associated with the stretching vibrations of methyl, methylene and methine at 2800-3000 cm^{-1} indicates microplastic weathering due to polymer oxidation (Dong et al., 2020).

The carbonyl index, a ratio between the peaks associated with C═O and CH_3 stretching, measured at 1716 and 720 cm^{-1}, respectively, is often used to quantify surface oxidation during polymer weathering (Almond et al., 2020; Liu and Yang, 2020). An increasing trend in the carbonyl index was observed with the increase in weathering. For PPE, the carbonyl index increased from 0.05 to 0.3 at the highest weathering condition while, for HDPE, the increase was from 0.02 to 0.11 (Fig. 2C). Large error bars are observed in the carbonyl index of aged plastics but not for pristine samples. This variation is due to the heterogeneous size distribution of the samples, which resulted in different oxidation rates for particles of different size. Nevertheless, a significant ($p \leq 0.05$) increase in the carbonyl index for both samples after 4 h of UV and H_2O_2 exposure indicates successful weathering of the microplastics. The carbonyl indices measured in this study are found to be in range of carbonyl indices measured in environmental microplastics (Sarkar et al., 2021; ter Halle et al., 2017; Veerasingam et al., 2016) as observed in Fig. 2D, although in the lower end of the values reported. This can be explained by the difference in aging time between laboratory and environmental samples, which have been exposed to environmental conditions for potentially years to decades. The aged microplastics produced by our accelerated weathering method can be described as young microplastics when compared to environmental samples.

Microplastics' weathering was further characterized by XPS to better understand the change in surface chemistry for each aging condition. Table 1 shows the oxygen and carbon content obtained from the wide-scan XPS analysis. Surface oxidation can be determined by the increase in oxygen content and decrease in carbon to oxygen (C/O) ratio with increasing aging conditions. From XPS analyses, both aging conditions were found to result in a similar degree of surface oxygen content; however, the initial oxygen content in HDPE was lower than in PPE, making the change in surface oxygen content greater for this microplastic. The aging trend observed in the XPS measurement differ slightly from the one observed by FT-IR with the carbonyl index, which can be attributed to the different penetration depths of each analytical technique. However, both measurements confirm the increasing oxidation of the microplastics in the order 0h < 4 h < 4 h + H_2O_2. It should be noted that oxygen is not a part of the chemical structure of pristine HDPE or PPE. Therefore, the oxygen measured in the pristine materials may be due to polymer damage during the blending process, residual water resulting from air exposure or incomplete drying, or additives (fillers, plasticizers, antioxidants, etc) found in the commercial plastics (da Costa et al., 2016).

To verify the nature of the surface oxidation, the C1s peak was deconvoluted. The C1s deconvolution of the microplastics (Fig. 3A–F) identified that there was indeed an increasing number of carbon-oxygen

Table 1
Carbon and oxygen content in the pristine and aged microplastics obtained through wide-scan XPS analyses (n = 3).

Samples	Wide-Scan elemental content		
	C (%)	O (%)	C/O
HDPE 0 h	96.20	3.75	25.65
HDPE 4 h	88.47	11.53	7.67
HDPE 4 h + H_2O_2	86.60	13.40	6.46
PPE 0 h	91.20	7.80	11.69
PPE 4 h	87.51	12.49	7.01
PPE 4 h + H_2O_2	87.00	13.00	6.69

functional groups, primarily hydroxyl and ether groups, after aging with UV light or UV + H_2O_2. These degradation products are in agreement with the photo- and oxo-degradation mechanisms of HDPE and PPE, which typically leads to the formation of C–OH and C–O–C functional groups (Benítez et al., 2013). The mechanisms involved in the formation of oxidation products in PPE during UV/O_3 treatment were described by Macmanus as a two-step process starting with (1) the insertion of O(^{1}D) atom to form ether and hydroxyl linkages that ultimately result in ether and hydroxyl groups, followed by (2) the hydrogen abstraction by O(^{3}P) that forms carbonyl groups via crosslinking (Macmanus, 1998). The C1s deconvolution support this mechanism by identifying these functional groups on the microplastics.

The effect of surface oxidation on the surface charge was also characterized to understand how aging can alter the interactions of microplastics with contaminants. For both microplastics, aging resulted in a change of the zeta potential towards less negative values (Figure S3 A-B). This change is attributed to the type of oxygen functional groups introduced, namely hydroxyl, ether, and carbonyl groups, which are all protonated and uncharged at neutral pH, contributing to a more neutral charge on the surface. Zeta potential values for both aged microplastics were similar to the ones reported for experimentally aged polystyrene microplastics (Sarkar et al., 2021). The addition of oxygen-containing functional groups to the surface, due to their polar nature, resulted in a trend towards higher hydrophilicity and surface free energy for both HDPE and PPE. This change was assessed using pristine and aged flat coupons of the same plastic material, due to the limitation of measuring contact angle on a powder of heterogeneous size distribution, and the data is shown in Figure S4.

3.3. Change in surface area and porosity during microplastics aging

The specific surface area (SSA) for both microplastics are summarized in Table 2. The data shows that SSA slightly decreased with aging in the case of as-prepared (i.e., unsieved) microplastics. For example, the SSA of PPE decreases from 0.025 m^2/g to 0.021 m^2/g after 4 h of aging with UV + H_2O_2 (Table 2). A similar observation of decreasing SSA in aged microplastics was shown by Sarkar et al. for polystyrene particles, which they attributed to the formation of carbonyl groups that can occupy the sites available for krypton adsorption during B.E.T. measurements (Sarkar et al., 2021). However, it should be noted that the SSA values obtained were below the detection limit of the instrument (0.05 m^2/g), indicating that the differences in SSA measured are small. To increase the krypton adsorption signal, measurements were performed with sieved microplastic where the largest particle fraction (collected on sieve #18) was removed, resulting in a smaller average particle size for the sample. The SSA of these sieved samples are shown in Table 2. The SSA of the sieved samples, as expected, is higher than the unsieved samples and on the contrary showed an increasing trend with the aging; however, the SSA values are still low and close or below the limit of detection. Overall, the data shown in Table 2 suggests that SSA may tend to increase with aging, based on the sieved samples results, but that the magnitude of the change was not significant enough to change the bulk SSA of the whole unsieved sample.

Table 2
Specific surface areas obtained for both microplastics under krypton adsorption. Values were obtained from one sample totaling ~10 g of dry microplastic powder.

Plastic Type	Aging Conditions	S_{BET} (m^2/g) (unsieved)	S_{BET} (m^2/g) (sieved)
HDPE	0 h	0.025	0.029
	4 h	0.019	0.037
	4 h with H_2O_2	Not Detected	0.036
PPE	0 h	0.025	0.052
	4 h	0.015	0.056
	4 h with H_2O_2	0.021	0.053

Given the low SSA values obtained by B.E.T. measurements, an alternative approach was used to understand if aging increased the SSA of microplastics. Fig. 4 shows the 3-D reconstructed X-ray tomography images of pristine (0 h) and aged (4 h with H_2O_2) HDPE microplastics. Formation of cracks can be seen for both pristine and aged microplastics, which are present only at the surface and converging few microns deep towards the center. A similar observation was found regarding crack formation for real environmental microplastics by (Halle et al., 2016). No internal porosity was observed. The surface porosity was calculated by taking a ratio of the crack volume or the defect volume on the selected ROI (Fig. 4B and D) to the total volume of ROI. Both the crack volume and total volume of ROIs were determined using foam analysis on the ROI. The total pore volume for pristine HDPE was 2.4% ± 0.6%, whereas the total pore volume for aged HDPE was 1.5% ± 0.2%, with no statistical difference between the two samples, as determined by a student t-test ($p \geq 0.05$). The X-ray tomography results confirm that porosity, and consequently surface area, did not change significantly after microplastic aging for microplastics size >1 mm which is also concurrent with the findings from a study done with microplastics fiber nets of size 1 mm and 10 mm found in real environment, where the surface area didn't change significantly.

3.4. Change in adsorption affinity of microplastics during aging

Adsorption isotherms were generated to understand how aging of microplastics can change their affinity for organic contaminants. Fig. 5 panels, 5A and 5B show the adsorption isotherms of pristine and aged HDPE microplastics with MB and phenanthrene. A stark 2.0–4.7-fold increase can be seen in the adsorbed amount of MB on HDPE microplastics (Fig. 5A) while, for phenanthrene, this increase is of 1.5–1.9-fold (Fig. 5B) when the pristine and 4h UV + H_2O_2 materials are compared. Similar results were obtained for the adsorption of MB and phenanthrene on PPE microplastics (Fig. 5C and D). It can be noted that phenanthrene adsorbs more onto microplastics compared to MB which may be attributed to its high hydrophobicity (Wang and Wang, 2018a). The phenanthrene isotherms also have a steeper slope, which suggest that there are higher energy and lower energy adsorption sites located heterogeneously on the surface of microplastics whereas, for MB, the less steep isotherms slope suggest that adsorption was more homogenous.

Several adsorption pathways have been described for the interaction of microplastics with organic contaminants, namely hydrophobic interactions, electrostatic interactions, hydrogen bonding, van der Waals forces and, π-π interactions (Torres et al., 2021). MB is known to protonate or deprotonate depending upon the pH, with a pK_a of 3.8, making MB cationic at the neutral pH used for adsorption. The cationic MB specie has been shown to interact with protonated oxygen functional groups, like phenol and ketones, on surfaces through H-bonding (Giraldo et al., 2021). Therefore, the higher surface oxygen content in aged microplastics can provide more interaction sites for the adsorption of MB.

On the other hand, phenanthrene, a neutral and hydrophobic (K_{ow} = 4.5) compound, mainly interacts through hydrophobic interactions (Wang and Wang, 2018a, 2018b). As such, the increase in phenanthrene adsorption after microplastic aging is not as pronounced compared to MB, as a hydrophobic compound is less likely to attach on the more hydrophilic aged surface. However, despite this unfavorable interaction, phenanthrene adsorption is still increased by aging in both PPE and HDPE (Fig. 5). The increase in adsorption may be associated with an increase in surface roughness that is not captured by the B.E.T. and X-ray tomography analyses realized (Wang et al., 2018). Weathering of microplastics by UV light also induces more fragmentation at lower size ranges, thereby generating newer submicron sized surfaces having higher surface areas (Song et al., 2017). This hypothesis is supported by the increasing trend in SSA for the sieved (<1 mm) microplastics in the B.E.T analysis. However, a role of surface chemistry cannot be ruled out

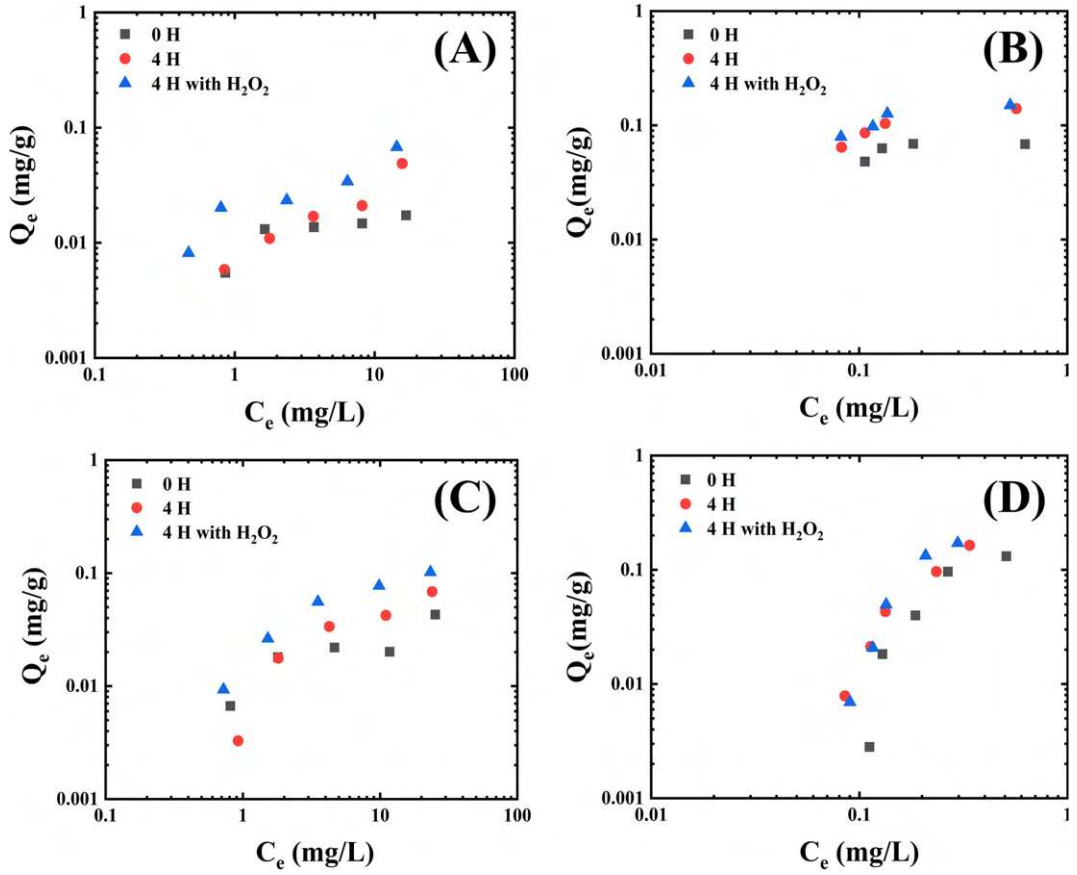

Fig. 5. Adsorption isotherms of (A) MB and (B) phenanthrene onto pristine and aged HDPE microplastics, and (C) MB and (D) phenanthrene onto pristine and aged PPE microplastics. The isotherms are presented as an average of three independent replicates (n = 3) on a log-normalized scale.

since the increase in adsorption is found in the bulk, unsieved microplastic samples that do not show evident change in SSA or surface roughness. In addition, the change in adsorption is not proportional to the change in SSA, even when compared to the sieved microplastic samples.

To better understand the adsorption of these contaminants on microplastics, adsorption isotherms were modelled using Langmuir or Freundlich models (Zhan et al., 2016), with the results shown in Table S3. Both microplastics show a better fitting for the Langmuir model, which suggests that the adsorption of contaminants onto HDPE and PPE is a single-layer adsorption process (Swenson and P. Stadie, 2019). In a study of the adsorption of antibiotics by pristine and aged polylactide (PLA) and polyvinyl chloride (PVC) microplastics, Fan et al. concluded that the enhanced adsorption found for aged microplastics can be related to changes in SSA, surface structure, surface charge, and presence of oxygen functional groups (Fan et al., 2021). Another study showed the enhanced adsorption of amlodipine (K_{ow} = 3) on polystyrene microplastics aged using photo-Fenton reaction. This study suggested that surface area and oxygen-containing functional groups were the dominant factors responsible for the increase in amlodipine to aged polystyrene, with chemical interactions like hydrogen bonding and electrostatic interactions becoming more important with aging (Liu et al., 2020). Similar mechanisms may be involved for the adsorption of phenanthrene to aged HDPE and PPE in the present study.

4. Conclusion

In this study, we developed a lab-based model for environmentally relevant microplastics, which was used to investigate how microplastic aging affects their interactions with organic contaminants. Microplastic aging was found to increase the affinity of microplastics with MB and phenanthrene, a phenomenon explained by the change in surface chemistry and surface area during aging. The effect of aging on adsorption to microplastics was different for the two organic contaminants, with higher increase in adsorption for MB due to their ability to interact with oxygen functional groups on the aged surface. The results of this study emphasize the need to better understand both the change in surface chemistry of microplastics during environmental weathering but also how this change will influence organic contaminant adsorption. The microplastic model developed in this study represents an early stage of microplastic aging, which raises important questions as to how more aged microplastics, as found after decades in the environment, will interact with organic contaminants. Given the potential role of microplastics as vectors of contaminants in the environment, understanding the complex interplay between surface weathering and contaminant adsorption will be critical in our capacity to assess future environmental risks posed by microplastic pollution.

Credit author statement

Kartik Bhagat: Conceptualization, Data curation, Formal analysis, Investigation, Methodology, Project administration, Software, Visualization. Writing-original draft, Writing-review and editing. **Ana C. Barrios**: Formal analysis, Software, Validation. Kimya Rajwade: Investigation, Methodology. **Abhishek Kumar**: Investigation, Methodology. **Jay Oswald**: Conceptualization, Project administration, Validation, Funding acquisition. **Onur Apul**: Conceptualization, Project administration, Validation, Supervision, Investigation, Funding acquisition, Writing-review and editing. **Francois Perreault**: Conceptualization, Data curation, Formal analysis, Project administration,

Visualization, Writing-review and editing, Validation, Resources, Supervision, Funding acquisition.

Declaration of competing interest

The authors declare that they have no known competing financial interests or personal relationships that could have appeared to influence the work reported in this paper.

Acknowledgement

Authors thankfully acknowledge the financial support from the National Science Foundation through the ECS 2003859 and 2004160 awards. We acknowledge the use of characterization facilities within the LeRoy Eyring Center for Solid State Science at Arizona State University and the technical assistance of Dr. Emmanuel Soignard, Dr. Douglas Daniel, and Dr. Timothy Karcher. We are thankful Dr. Leila Ladani and Dr. Maryam Sadeghilaridjani for providing us X-Ray tomography data. We are also thankful to Sam Callandar and Ivan Moreno from the Volume Graphics technical support team for providing a publishable image for our tomography results. Finally, we are grateful to Dr. Brian Frederick at the University of Maine for B.E.T. analysis.

Appendix A. Supplementary data

Supplementary data to this article can be found online at https://doi.org/10.1016/j.chemosphere.2022.134238.

References

Almond, J., Sugumaar, P., Wenzel, M.N., Hill, G., Wallis, C., 2020. Determination of the carbonyl index of polyethylene and polypropylene using specified area under band methodology with ATR-FTIR spectroscopy. E-Polymers 20, 369–381. https://doi.org/10.1515/epoly-2020-0041.

Álvarez-Ruiz, R., Picó, Y., Campo, J., 2021. Bioaccumulation of emerging contaminants in mussel (Mytilus galloprovincialis): influence of microplastics. Sci. Total Environ. 796 https://doi.org/10.1016/j.scitotenv.2021.149006.

Andrady, A.L., 2011. Microplastics in the marine environment. Mar. Pollut. Bull. 62, 1596–1605. https://doi.org/10.1016/j.marpolbul.2011.05.030.

Andreassen, E., 1999. Infrared and Raman Spectroscopy of Polypropylene, pp. 320–328. https://doi.org/10.1007/978-94-011-4421-6_46.

Bakir, A., Rowland, S.J., Thompson, R.C., 2012. Competitive sorption of persistent organic pollutants onto microplastics in the marine environment. Mar. Pollut. Bull. 64, 2782–2789. https://doi.org/10.1016/j.marpolbul.2012.09.010.

Bakir, A., Rowland, S.J., Thompson, R.C., 2014. Transport of persistent organic pollutants by microplastics in estuarine conditions. Estuar. Coast Shelf Sci. 140, 14–21. https://doi.org/10.1016/j.ecss.2014.01.004.

Barnes, D.K.A., Galgani, F., Thompson, R.C., Barlaz, M., 2009. Accumulation and fragmentation of plastic debris in global environments. Phil. Trans. Biol. Sci. 364, 1985–1998. https://doi.org/10.1098/rstb.2008.0205.

Benítez, A., Sánchez, J.J., Arnal, M.L., Müller, A.J., Rodríguez, O., Morales, G., 2013. Abiotic degradation of LDPE and LLDPE formulated with a pro-oxidant additive. Polym. Degrad. Stabil. 98, 490–501. https://doi.org/10.1016/j.polymdegradstab.2012.12.011.

Bhagat, J., Nishimura, N., Shimada, Y., 2021. Toxicological interactions of microplastics/nanoplastics and environmental contaminants: current knowledge and future perspectives. J. Hazard Mater. 405 https://doi.org/10.1016/j.jhazmat.2020.123913.

Brandon, J., Goldstein, M., Ohman, M.D., 2016. Long-term aging and degradation of microplastic particles : comparing in situ oceanic and experimental weathering patterns. MPB 110, 299–308. https://doi.org/10.1016/j.marpolbul.2016.06.048.

Cole, M., Lindeque, P., Halsband, C., Galloway, T.S., 2011. Microplastics as contaminants in the marine environment: a review. Mar. Pollut. Bull. 62, 2588–2597. https://doi.org/10.1016/j.marpolbul.2011.09.025.

da Costa, J.P., Santos, P.S.M., Duarte, A.C., Rocha-Santos, T., 2016. (Nano)plastics in the environment - sources, fates and effects. Sci. Total Environ. 566-567 (1), 15–26. https://doi.org/10.1016/j.scitotenv.2016.05.041.

Desforges, J.P.W., Galbraith, M., Dangerfield, N., Ross, P.S., 2014. Widespread distribution of microplastics in subsurface seawater in the NE Pacific Ocean. Mar. Pollut. Bull. 79, 94–99. https://doi.org/10.1016/J.MARPOLBUL.2013.12.035.

Dong, M., Zhang, Q., Xing, X., Chen, W., She, Z., Luo, Z., 2020. Raman spectra and surface changes of microplastics weathered under natural environments. Sci. Total Environ. 739. https://doi.org/10.1016/j.scitotenv.2020.139990.

Eriksen, M., Maximenko, N., Thiel, M., Cummins, A., Lattin, G., Wilson, S., Hafner, J., Zellers, A., Rifman, S., 2013. Plastic pollution in the South Pacific subtropical gyre. Mar. Pollut. Bull. 68, 71–76. https://doi.org/10.1016/J.MARPOLBUL.2012.12.021.

Fan, X., Zou, Y., Geng, N., Liu, J., Hou, J., Li, D., Yang, C., Li, Y., 2021. Investigation on the adsorption and desorption behaviors of antibiotics by degradable MPs with or without UV ageing process. J. Hazard Mater. 401, 123363 https://doi.org/10.1016/J.JHAZMAT.2020.123363.

Gajšt, T., Bizjak, T., Palatinus, A., Liubartseva, S., Kržan, A., 2016. Sea surface microplastics in slovenian part of the northern adriatic. Mar. Pollut. Bull. 113, 392–399. https://doi.org/10.1016/J.MARPOLBUL.2016.10.031.

Gesamp, 2015. Sources, fate and effects of microplastics in the marine environment: a global assessmen. In: Kershaw, P.J. (Ed.), IMO/FAO/UNESCOIOC/UNIDO/WMO/IAEA/UN/UNEP/UNDP Joint Group of Experts on the Scientific Aspects of Marine Environmental Protection), vol. 90. Rep. Stud. GESAMP, p. 96.

Geyer, R., Jambeck, J.R., Law, K.L., 2017. Production, use, and fate of all plastics ever made. Sci. Adv. 3, e1700782 https://doi.org/10.1126/sciadv.1700782.

Giraldo, S., Robles, I., Godínez, L.A., Acelas, N., Flórez, E., 2021. Experimental and theoretical insights on methylene blue removal from wastewater using an adsorbent obtained from the residues of the orange industry. Molecules 26. https://doi.org/10.3390/molecules26154555.

Halle, A., Ladirat, L., Gendre, X., Goudouneche, D., Pusineri, C., Routaboul, C., Tenailleau, C., Duployer, B., Perez, E., 2016. Understanding the Fragmentation Pattern of Marine Plastic Debris. https://doi.org/10.1021/acs.est.6b00594.

Halle, A., Ladirat, L., Martignac, M., Mingotaud, A.F., Boyron, O., Perez, E., 2017. To what extent are microplastics from the open ocean weathered? Environ. Pollut. 227, 167–174. https://doi.org/10.1016/j.envpol.2017.04.051.

Hameed, B.H., Ahmad, A.L., Latiff, K.N.A., 2007. Adsorption of basic dye (methylene blue) onto activated carbon prepared from rattan sawdust. Dyes Pigments 75, 143–149. https://doi.org/10.1016/j.dyepig.2006.05.039.

Hüffer, T., Weniger, A., Hofmann, T., 2018. Sorption of organic compounds by aged polystyrene microplastic. Environ. Pollut. 236, 218–225. https://doi.org/10.1016/j.envpol.2018.01.022.

Kanhai, L.D.K., Officer, R., Lyashevska, O., Thompson, R.C., O'Connor, I., 2017. Microplastic abundance, distribution and composition along a latitudinal gradient in the Atlantic Ocean. Mar. Pollut. Bull. 115, 307–314. https://doi.org/10.1016/J.MARPOLBUL.2016.12.025.

Klein, S., Worch, E., P Knepper, T., 2015. Occurrence and spatial distribution of microplastics in river shore sediments of the rhine-main area in Germany. Environ. Sci. Technol. 49, 6070–6076. https://doi.org/10.1021/acs.est.5b00492.

Koelmans, A.A., Bakir, A., Burton, G.A., Janssen, C.R., 2016. Microplastic as a vector for chemicals in the aquatic environment: critical review and model-supported reinterpretation of empirical studies. Environ. Sci. Technol. 50, 3315–3326. https://doi.org/10.1021/acs.est.5b06069.

Lee, H., Shim, W.J., Kwon, J.H., 2014. Sorption capacity of plastic debris for hydrophobic organic chemicals. Sci. Total Environ. 470–471, 1545–1552. https://doi.org/10.1016/j.scitotenv.2013.08.023.

Liu, X., Yang, R., 2020. Conversion among photo-oxidative products of polypropylene in solid, liquid and gaseous states. BMC Chemistry 14. https://doi.org/10.1186/s13065-020-00698-y.

Liu, P., Lu, K., Li, J., Wu, X., Qian, L., Wang, M., Gao, S., 2020. Effect of aging on adsorption behavior of polystyrene microplastics for pharmaceuticals: adsorption mechanism and role of aging intermediates. J. Hazard Mater. 384, 121193 https://doi.org/10.1016/J.JHAZMAT.2019.121193.

Lowry, G., Field, J., Westerhoff, P., Zimmerman, J., Alvarez, P., Boehm, A., Crittenden, J., Dachs, J., Diamond, M., Eckelman, M., Gardea-Torresdey, J., Giammar, D., Hofstetter, T., Hornbuckle, K., Jiang, G., Li, X., Leusch, F., Mihelcic, J., Miller, S., Pruden, A., Raskin, L., Richardson, S., Scheringer, M., Schlenk, D., Strathmann, T., Tao, S., Waite, T.D., Wang, P., Wang, S., 2020. Why was my paper rejected without review? Environ. Sci. Technol. 54, 11641–11644. https://doi.org/10.1021/acs.est.0c05784.

Macmanus, L.F., 1998. Thesis on Surface Modification Studies of Polypropylene Using Ultraviolet Radiation and Ozone. National Library of Canada.

Ngoc, N., Zalouk-vergnoux, A., Poirier, L., Mouneyrac, C., Lagarde, F., 2016. Is There Any Consistency between the Microplastics Found in the Fi Eld and Those Used in Laboratory Experiments ? * 211. https://doi.org/10.1016/j.envpol.2015.12.035.

Pandey, J.K., Singh, R.P., 2001. Uv-irradiated biodegradability of ethylene-propylene copolymers, LDPE, and I-PP in composting and culture environments. Biomacromolecules 2, 880–885. https://doi.org/10.1021/bm010047s.

Revel, M., Châtel, A., Mouneyrac, C., 2018. Micro(nano)plastics: a threat to human health? Current Opinion in Environmental Science and Health 1, 17–23. https://doi.org/10.1016/j.coesh.2017.10.003.

Ritchie, H., Roser, M., 2018. Plastic Pollution. Published online at OurWorldInData.org. https://ourworldindata.org/plastic-pollution'.

Rubin, A.E., Zucker, I., 2022. Interactions of microplastics and organic compounds in aquatic environments: a case study of augmented joint toxicity. Chemosphere 289, 133212. https://doi.org/10.1016/J.CHEMOSPHERE.2021.133212.

Rubin, A.E., Sarkar, A.K., Zucker, I., 2021. Questioning the suitability of available microplastics models for risk assessment – a critical review. Sci. Total Environ. 788, 147670 https://doi.org/10.1016/j.scitotenv.2021.147670.

Sarkar, A.K., Rubin, A.E., Zucker, I., 2021. Engineered polystyrene-based microplastics of high environmental relevance. Environ. Sci. Technol. 55, 10491–10501. https://doi.org/10.1021/acs.est.1c02196.

Setälä, O., Fleming-lehtinen, V., Lehtiniemi, M., 2014. Ingestion and transfer of microplastics in the planktonic food web. Environ. Pollut. 185, 77–83. https://doi.org/10.1016/j.envpol.2013.10.013.

Song, Y.K., Hong, S.H., Jang, M., Han, G.M., Jung, S.W., Shim, W.J., 2017. Combined Effects of UV exposure duration and mechanical abrasion on microplastic fragmentation by polymer type. Environ. Sci. Technol. 51 (8), 4368–4376. https://doi.org/10.1021/acs.est.6b06155.

Swenson, H., P Stadie, N., 2019. Langmuir's theory of adsorption: a centennial review. Langmuir 35, 5409–5426. https://doi.org/10.1021/acs.langmuir.9b00154.

Teuten, E.L., Saquing, J.M., Knappe, D.R.U., Barlaz, M.A., Jonsson, S., Björn, A., Rowland, S.J., Thompson, R.C., Galloway, T.S., Yamashita, R., Ochi, D., Watanuki, Y., Moore, C., Viet, P.H., Tana, T.S., Prudente, M., Boonyatumanond, R., Zakaria, M.P., Akkhavong, K., Ogata, Y., Hirai, H., Iwasa, S., Mizukawa, K., Hagino, Y., Imamura, A., Saha, M., Takada, H., 2009. Transport and release of chemicals from plastics to the environment and to wildlife. Phil. Trans. Biol. Sci. 364, 2027–2045. https://doi.org/10.1098/rstb.2008.0284.

Thompson, Richard C., Olsen, Ylva, Mitchell, Richard P., Davis, Anthony, Rowland, Steven J., John, Anthony W.G., McGonigle, Daniel, Russell, Andrea E., 2004. Lost at sea: where is all the plastic? Science 304, 838. https://doi.org/10.1126/science.1094559.

Torres, F.G., Dioses-Salinas, D.C., Pizarro-Ortega, C.I., De-la-Torre, G.E., 2021. Sorption of Chemical Contaminants on Degradable and Non-degradable Microplastics: Recent Progress and Research Trends. Science of the Total Environment. https://doi.org/10.1016/j.scitotenv.2020.143875.

Veerasingam, S., Saha, M., Suneel, V., Vethamony, P., Rodrigues, A.C., Bhattacharyya, S., Naik, B.G., 2016. Characteristics, seasonal distribution and surface degradation features of microplastic pellets along the Goa coast, India. Chemosphere 159, 496–505. https://doi.org/10.1016/j.chemosphere.2016.06.056.

Vroom, R.J.E., Koelmans, A.A., Besseling, E., Halsband, C., 2017. Aging of microplastics promotes their ingestion by marine. Environ. Pollut. 231, 987–996. https://doi.org/10.1016/j.envpol.2017.08.088.

Wang, W., Wang, J., 2018a. Ecotoxicology and Environmental Safety Di ff erent partition of polycyclic aromatic hydrocarbon on environmental particulates in freshwater : microplastics in comparison to natural sediment. Ecotoxicol. Environ. Saf. 147, 648–655. https://doi.org/10.1016/j.ecoenv.2017.09.029.

Wang, W., Wang, J., 2018b. Chemosphere Comparative evaluation of sorption kinetics and isotherms of pyrene onto microplastics. Chemosphere 193, 567–573. https://doi.org/10.1016/j.chemosphere.2017.11.078.

Wang, Z., Chen, M., Zhang, L., Wang, K., Yu, X., Zheng, Z., Zheng, R., 2018. Sorption behaviors of phenanthrene on the microplastics identi fi ed in a mariculture farm in Xiangshan Bay , southeastern China. Sci. Total Environ. 628–629, 1617–1626. https://doi.org/10.1016/j.scitotenv.2018.02.146.

Worm, B., Lotze, H.K., Jubinville, I., Wilcox, C., Jambeck, J., 2017. Plastic as a persistent marine pollutant. Annu. Rev. Environ. Resour. 42, 1–26. https://doi.org/10.1146/annurev-environ-102016-060700.

Wright, S.L., Thompson, R.C., Galloway, T.S., 2013. The Physical Impacts of Microplastics on Marine Organisms: a Review. Environmental Pollution (Barking, Essex : 1987). https://doi.org/10.1016/j.envpol.2013.02.031.

Wypych, G., 2013. Artificial weathering versus natural exposure. In: Handbook of Material Weathering. Elsevier, pp. 231–244. https://doi.org/10.1016/b978-1-895198-62-1.50014-7.

Zhan, Z., Wang, J., Peng, J., Xie, Q., Huang, Y., Gao, Y., 2016. Sorption of 3,3',4,4'-tetrachlorobiphenyl by microplastics: a case study of polypropylene. MPB 110, 559–563. https://doi.org/10.1016/j.marpolbul.2016.05.036.